

# Mechanism on epoxidation of alkenes by peracids: A protonation-promoted pathway and its quantum chemical elucidation

Hongchang Shi<sup>\*</sup>, Zhiguo Zhang, Yilui Wang

*Department of Chemistry, Tsinghua University, Beijing 100084, China*

Received 21 September 2004; received in revised form 22 April 2005; accepted 23 April 2005

Available online 13 June 2005

## Abstract

By a density functional theory (DFT) based quantum chemical calculation at the B3LYP/6-311G(d,p) level, we found that the mechanism of epoxidation of alkenes by peracids is a protonation-promoted pathway. The protonation site is the oxygen atom of carbonyl group in peracids. Orbital energy  $E_{UMO\sigma^*}$  of the UMO in which the  $\sigma^*$  orbital of peroxy bond of protonated peracids lies is much lower than that of neutral peracids. The  $E_{UMO\sigma^*}$  are in the range of  $-6.21$  to  $-7.96$  eV, which is  $5-7$  eV lower than that of neutral peracids. The  $E_{UMO\sigma^*}$  is in the same as or even lower level than the HOMO energy of alkenes. The study first exhibits the images of  $\sigma^*$  orbital of the peroxy bonds in neutral or protonated peroxy acids. A reaction path calculation (IRC) revealed that the microscopic process of the epoxidation by peracids is a nucleophilic transfer of  $\pi$ -electrons of alkene toward the  $\sigma^*$  orbital of peroxy bond. The calculation has given the transition structures (TS) and activation barriers to the attack of epoxidation of performic acid, peracetic acid, trifluoroperacetic acid and their protonated counterparts on ethylene. Their activation barriers are 17.51, 19.18, 13.93, 3.18, 4.25, and 2.77 kcal/mol, respectively, showing that the protonation greatly dropped the activation barriers of epoxidation by peracids, i.e. the neutral peracids were strongly activated by the protonation. According to this mechanism, some important and puzzling kinetic facts of epoxidation by peracids are easily elucidated.

© 2005 Elsevier B.V. All rights reserved.

**Keywords:** Epoxidation; Quantum chemistry; Peracid; Protonation;  $\sigma^*$  orbital

## 1. Introduction

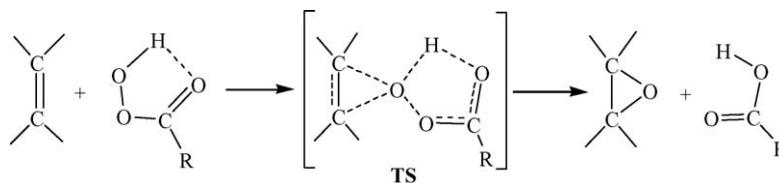
Peracids react directly with alkenes to provide the corresponding epoxides, which has always been a useful and convenient way. The commonly accepted mechanism of the epoxidation first proposed by Bartlett [1] involves nucleophilic attack of the  $\pi$ -electrons of double bond at the terminal electrophilic oxygen atom of the hydroperoxide group where the proton is transferred intramolecularly to the carbonyl oxygen simultaneously (Scheme 1). Because of the unique planar transition structure (TS), it is often referred to as the “butterfly mechanism”. According to this mechanism, the epoxidation is carried out by neutral peracids. Although the mechanism has been widely accepted, it also comes across serious difficulties often. For example, it is unable to

explain the diverse catalytic or retarding role of other acids on the epoxidations of some alkenes, which often causes people to be puzzled [2].

Over 50 years, many chemists have conducted a number of experimental and theoretical studies [3] on the epoxidation mechanism, including quantum chemical studies [4]. However, almost all the studies are an elongation or improvement on the Bartlett model, i.e. all assume that completion of the epoxidation is dependent on neutral peracids. Therefore, the studies on the mechanism of alkene epoxidation by peracids have not achieved essential progress or breakthrough.

Our recently quantum chemical study with the DFT method revealed the Bartlett pathway is quite questionable. The calculation result and some experimental facts show that neutral peracids are hard to complete the epoxidation. The epoxidation of olefins by peracids should be a protonation-promoted pathway. The protonation on the carbonyl group in peracid is the key step in the epoxidation. The protonation

<sup>\*</sup> Corresponding author. Tel.: +86 1062783878; fax: +86 1062771149.  
E-mail address: [shihc@mail.tsinghua.edu.cn](mailto:shihc@mail.tsinghua.edu.cn) (H. Shi).



Scheme 1. Bartlett mechanism of the epoxidation of olefins by peracids.

greatly lowers the energy of  $\sigma^*$  orbital of the peroxy bond in peracids, and thus largely dropped the activation barriers of oxygen transfer toward alkenes, making the epoxidation easily initiated and completed.

## 2. Results and discussion

### 2.1. The calculation method

The calculation has been carried out with the Gaussian 98 [5] program package. Molecular orbitals (MO) and their energies of neutral or protonated peracids and alkenes, the geometries and energies of transition structures, single-point energy calculation, zero-point energy contribution (ZPE) and reaction path calculation (IRC) all have been calculated with DFT at the B3LYP/6-311G(d,p) level. We consider that using the same calculation method, level and basis set in the calculation is favorable for comparing the data and achieving dependable conclusion.

The calculation on some MOs, especially UMOs, occupies an important place in the study. The DFT/B3LYP method treats electron correlation energy well and so can effectively calculate the MOs and their energies. The 6-311G(d,p) basis set is a quite large one. The results obtained by the B3LYP/6-311G(d,p) indicated that the calculation precision is suitable for the mechanism study. At first, several other methods were also used for calculating the OMOs or UMOs. We found the calculation results are not suitable for explaining microscopic nature and experimental findings in the epoxidation. For example, Fig. 1 shows the graph and energy of the UMO in which the  $\sigma^*$  orbitals of neutral or protonated performic acid lie obtained with DFT at the B3LYP/6-311G(d,P) level and with *ab initio* at the MP2/6-31g(d,p) level. The four ellipsoids h, i, j and k in the graphs have the typical shape of an  $\sigma^*$  orbital. The graphs clearly show the  $\sigma^*$  orbital of peroxy bond is major component of the UMO. Therefore,  $E_{\text{UMO}\sigma^*}$  of the UMOs can reflect and represent the reactivity of an  $\sigma^*$  orbital. Among them, the graphs obtained by the DFT/B3LYP have better  $\sigma^*$  antibonding characteristics than that obtained by the *ab initio*/MP2. It is more important that  $E_{\text{UMO}\sigma^*}$  (-7.70 eV) of protonated performic acid obtained by the DFT/B3LYP method are much lower than that (-1.71 eV) obtained by the *ab initio*/MP2.  $E_{\text{UMO}\sigma^*}$  (-7.70 eV) is in the same level as  $E_{\text{MO}\pi}$  (-5.5 to -7.5 eV) of alkenes. The result can explain why the epoxidation of alkenes by peracids often was carried out at 0 °C or even lower temperature. It indicated

that the DFT/B3LYP method fairly well presented orbital graphs and energies of the UMOs in which the  $\sigma^*$  orbitals of neutral and protonated peracids lie.

In the last decade, the DFT method has become an important tool in clarifying mechanism of olefin epoxidation. A glaring example is that the longstanding controversy about the mechanism of olefin epoxidation with Mimonn-type diperoxomolybdenum complexes has been settled with the help of the DFT [6]. According to the mechanism, the epoxidation does not follow a stepwise pathway but a direct oxygen transfer process suggested by Sharpless that is already widespread approved. Therefore, in the study we have selected the DFT method for exploring the epoxidation mechanism of alkene by peracids.

### 2.2. The $\sigma^*$ orbital energies of neutral peracids are much higher than the $\pi$ orbital energies of alkenes

For the neutral peracids, the DFT calculation results at the B3LYP/6-311G(d, p) level are shown in Table 1 and Fig. 1. The integer  $N_{\text{UMO}\sigma^*}$  shows number of the UMO in which the  $\sigma^*$  orbital of peroxy bond of peracid lies. In Gaussian 98, the Numbers of MOs start from HOMO and LUMO and accord to the energy order. Both of the numbers ( $N_{\text{HOMO}}$ ,  $N_{\text{LUMO}}$ )

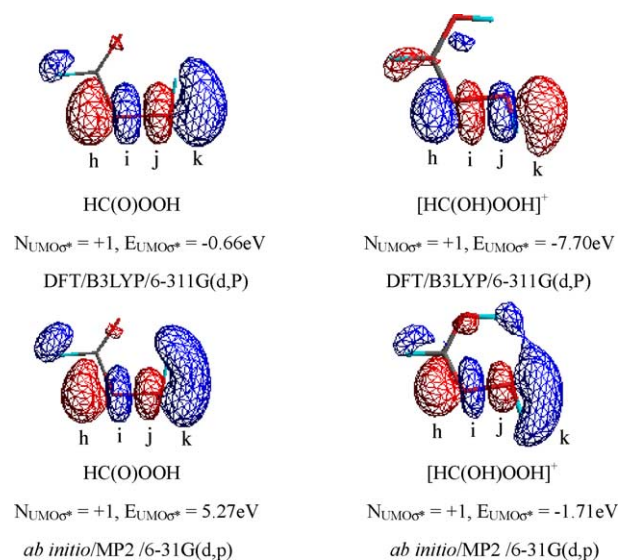
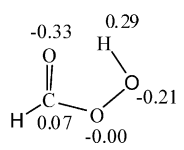
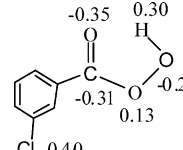
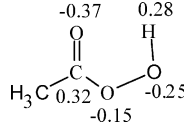
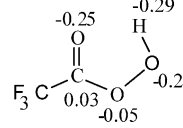
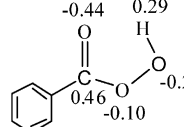


Fig. 1. The graphs and energies of the UMO in which  $\sigma^*$  orbital of peroxy bond of neutral and protonated performic acid lies obtained by DFT at the B3LYP/6-311G(d,p) level and by *ab initio* at the MP2/6-31G(d,p) level (orbital contour value = 0.05).

Table 1

$E_{UMO\sigma^*}$  and  $N_{UMO\sigma^*}$  of the UMOS in which the  $\sigma^*$  orbital of peroxy bond of neutral peracids lies and Mulliken atomic charges of some atoms calculated by DFT at the B3LYP/6–311G(d,p) level

Peracids	$N_{UMO\sigma^*}$	$E_{UMO\sigma^*}$ (eV)	Peracids	$N_{UMO\sigma^*}$	$E_{UMO\sigma^*}$ (eV)
	+1	-0.66		+2	-0.43
	+1	-0.26		+1	-1.31
	+2	-0.22			

of HOMO and LUMO are assigned to zero. The numbers  $N_{UMO}$  of other UMOS are positive integers. For example, the number of the UMO next to LUMO is +1. The numbers  $N_{OMO}$  of other OMOS are negative integers. For example, the number of the OMO next to HOMO is -1.

For performic acid and peracetic acid, the  $\sigma^*$  orbital of their peroxy bonds is in the UMOS with  $N_{UMO\sigma^*} = +1$ , but for PBA and mCPBA, their  $\sigma^*$  is in the UMOS with  $N_{UMO\sigma^*} = +2$  that should be attributed to the substitute groups in the molecules.  $E_{UMO\sigma^*}$  of the neutral peracids is in the range of -1.31 to -0.22 eV (Table 1, Fig. 2).

For alkenes, the calculation results indicate that the  $\pi$  orbital of double bond is the main component of HOMO of the molecules. Therefore, the energy  $E_{HOMO}$  of the HOMO can reflect and represent the reactivity of  $\pi$ -electrons of

the alkenes [7]. The energy  $E_{MO\pi}$  of the MO in which the  $\pi$ -orbital of alkenes lie are generally in range of -5.5 to -7.5 eV. Fig. 3 contains several examples. However, the energy difference between the  $E_{HOMO}$  of the alkenes and  $E_{UMO\sigma^*}$  of neutral peracids (Table 1) would amount to 5.0–7.0 eV (120–160 kcal/mol) that is a fairly great energy difference. This indicates that completing the oxygen transfer through nucleophilic attack of  $\pi$ -electrons of olefins toward the  $\sigma^*$  orbital of peroxy bond of neutral peracid must overcome quite high barriers. It would be difficult to complete the epoxidation by neutral peracids. However, the protonation of peroxy acids changes the situation.

### 2.3. The protonation of peracids

The protonation of neutral peracids can adopt several styles because all the three oxygens in  $-C(O)OOH$  have abil-

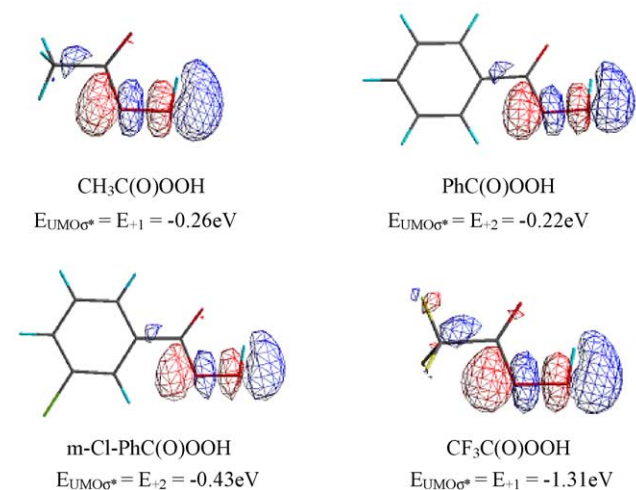


Fig. 2. Graphs and energies of the UMOS in which the  $\sigma^*$  orbital of peroxy bond of neutral peracids lies obtained by DFT at the B3LYP/6–311G(d,p) level. Orbital contour value = 0.05,  $HC(O)OOH$ , see Fig. 1.

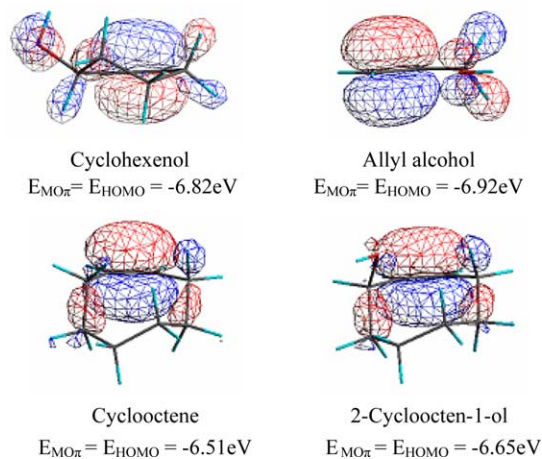
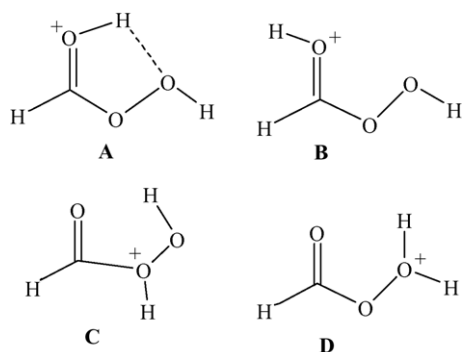


Fig. 3. Graphs and orbital energies of HOMOs of several alkenes obtained by DFT at the B3LYP/6–311G(d,p) level (orbital contour value = 0.05). The  $\pi$  orbitals of double bonds are the main component of the HOMOS.



Scheme 2. The isomers or conformers of the protonations on peracids.

ity and chance to combine with  $H^+$ . The most probable way is that  $H^+$  combines with carbonyl oxygen (Scheme 2, **A** and **B**) because there is the richest negative charge on the oxygen atom (Table 1). Bach et al. [4(a)] have conducted the study on the various isomers or conformers of protonated peroxyformic acid through the calculation with ab initio at the MP2/6-31G(d) or 6-31G(d,p) and with DFT at the B3LYP/6-311G(d,p) levels. Their calculation results at the B3LYP/6-311G(d,p) levels indicated the protonation of carbonyl oxygen atom is the most favorable because the proton affinity (PA) of the oxygen atom is 23.1 kcal/mol (at 0K) greater than that of its adjacent peroxy oxygen atom (isomer **C** in Scheme 2). Moreover, the syn-protonated conformer **A**, where the more acidic proton is hydrogen bonded to the hydroxyl oxygen, is 1.7 kcal/mol lower than the anti conformer **B** that lacks hydrogen bonding (Scheme 2). We calculated protonated isomer **D** at the B3LYP/6-311G(d,p) level. We found that the isomer **D** auto-changed into the conformer **A** as the optimization went on (Fig. 4). Therefore, we only consider conformer **A** in the following calculation.

The total energies ( $E$ ) of the protonated and neutral peracids obtained by the calculation at the RB3LYP/6-311G(d,p) level are shown in Table 2. The results indi-

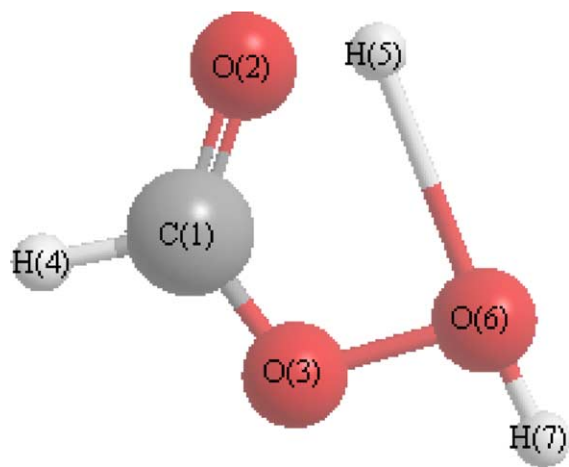


Fig. 4. Protonated isomer **D** auto-changed into conformer **A** as the optimization goes on at the B3LYP/6-311G(d,p) level.

cated that the protonation on carbonyl group makes the total energy has remarkably dropped down. The reduced quantity is precisely the proton affinity PA (160–210 kcal/mol). Therefore, protonated peracid is an intermediate that easily forms.

#### 2.4. The protonation greatly lowered the energy of $\sigma^*$ orbital of peroxy bond

When the peracids are in the protonated positive ion state, the  $\sigma^*$  orbital of peroxy bond is also the major component of a UMO. Therefore,  $E_{UMO\sigma^*}$  of the UMO can reflect and represent the reactivity of the  $\sigma^*$  orbital of peroxy bond in the protonated peracids. The calculation results at the RB3LYP/6-311G(d,p) level are shown in Table 2. Obviously,  $E_{UMO\sigma^*}$  of the UMO in which the  $\sigma^*$  orbital of peroxy bond lies is much lower than the orbital energy of the neutral acids. The  $E_{UMO\sigma^*}$  is in the range of  $-6.21$  to  $-7.97$  eV; i.e. 5–7 eV lower than that of the neutral peracids.  $E_{UMO\sigma^*}$  of protonated peracids are in the same as, or even lower level than the  $E_{MO\pi}$  of olefins (see Section 2). Therefore, the nucleophilic transfer of  $\pi$ -electrons of olefins toward the  $\sigma^*$  orbital of peroxy bond were easily completed even at low temperature. The graphs of the UMOs are shown in Fig. 5.

#### 2.5. The protonation greatly lowered the activation barriers of the epoxidation

By the DFT calculation at the B3LYP/6-311G(d,p) level, we have obtained the transition structures (Fig. 6, **TS a–f**) and energies (Table 3) of the attack of performic acid, peracetic acid, trifluoroperacetic acid and their protonated counterparts on a simple alkene–ethylene. The results indicated that the

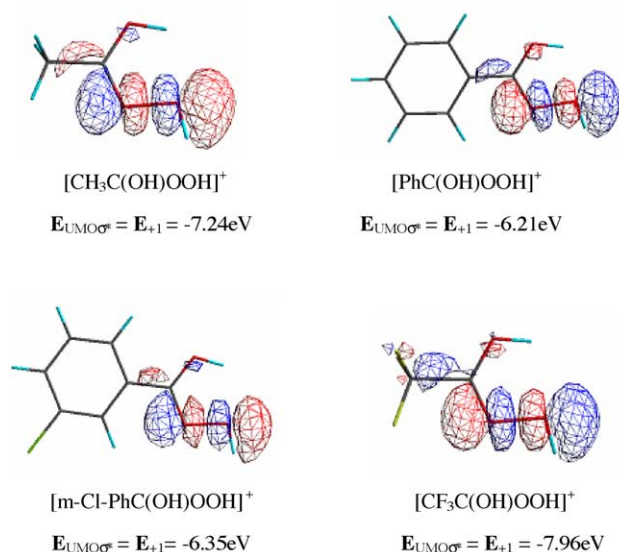


Fig. 5. Protonated peracids in conformer **A**: the graphs and energies of the UMOs in which the  $\sigma^*$  orbital of proxo bond lies (orbital contour value = 0.05. the graph and energy of  $[HC(OH)OOH]^+$  see Fig. 1).

Table 2

 $E_{\text{UMO}\sigma^*}$  of the UMOs in which the  $\sigma^*$  orbital of proxo bond lies and PA (298 k) of the protonated peroxy acids obtained at the B3LYP/6-311G(d,p) level

Protonated peracids	$E$ (a.u.)	PA (kcal/mol)	$N_{\text{UMO}\sigma^*}$	$E_{\text{UMO}\sigma^*}$ (eV)
	-265.260256 (-264.963270)	186.3	+1	-7.70
	-304.621045 (-304.302185)	200.0	+1	-7.24
	-496.413622 (-496.083834)	206.8	+1	-6.21
	-956.027118 (-955.703493)	203.0	+1	-6.35
	-602.353694 (-602.087714)	166.8	+1	-7.96

The value in parentheses is  $E_{\text{UMO}\sigma^*}$  of neutral peracids.

protonation has greatly reduced the activation barriers of transition structures. The optimized initiative structures (clusters) of neutral or protonated peracids on ethylene are left out in Fig. 6, but the energies and zero point correction energies (ZPE) of the systems are listed in Table 3 for calculating the energies of the activation barriers. If performic acid, peracetic acid and trifluoroperacetic acid are protonated, the activation barriers of the epoxidation on ethylene have dropped by 14.33, 14.93, and 11.16 kcal/mol, respectively. Under the acidic condition of the epoxidation by peracids, the protona-

tion would certainly occur. Therefore, the epoxidation would mainly be or even entirely carried out by the protonated peracids because they lead to much lower activation barriers than the neutral peracids. Of course, although neutral peracids have much higher activation barriers than protonated ones, we still do not have good grounds for absolutely excluding the possibility of epoxidation by neutral peracids.

The transition structures (TS--a-c) of the neutral peracids and that (TS--d-f) of their protonated counterparts in Fig. 6 have two remarkable differences:

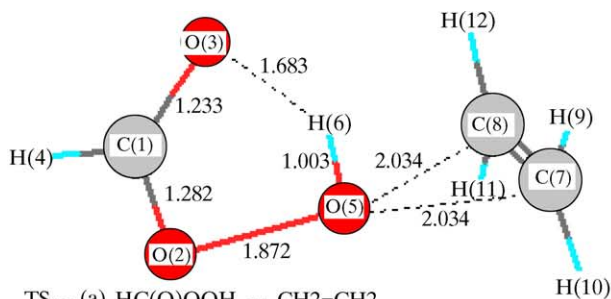
Table 3

Activation barriers obtained from electronic energies ( $E_{\text{TS}}$ ,  $E_{\text{cluster}}$ ), zero-point correction energies ( $ZPE_{\text{TS}}$ ,  $ZPE_{\text{cluster}}$ ) of clusters and transition structures (TS) of performic acid (a), peracetic acid (b), trifluoroperacetic acid (c) and their protonated counterparts (d-f) on ethylene

	$E_{\text{TS}}$ (a.u.)	$ZPE_{\text{TS}}$ (a.u.)	$E_{\text{cluster}}$ (a.u.)	$ZPE_{\text{cluster}}$ (a.u.)	$E^*$ (kcal/mol)
a	-343.553526	0.088666	-343.581636	0.088861	17.51 (17.63)
b	-382.888981	0.116236	-382.919807	0.116472	19.18 (19.33)
c	-680.684780	0.093599	-680.706899	0.093501	13.93 (13.87)
d	-343.888290	0.100129	-343.895243	0.102004	3.18 (4.36)
e	-383.240980	0.127755	-383.249101	0.129101	4.25 (5.09)
f	-681.000503	0.104182	-681.006791	0.106050	2.77 (3.94)

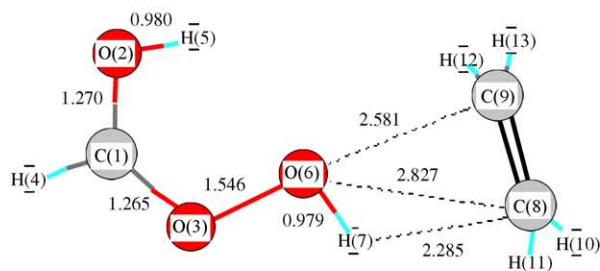
The data in parentheses do not consider the zero-point correction energies.



TS--- (a) HC(O)OOH --- CH<sub>2</sub>=CH<sub>2</sub>

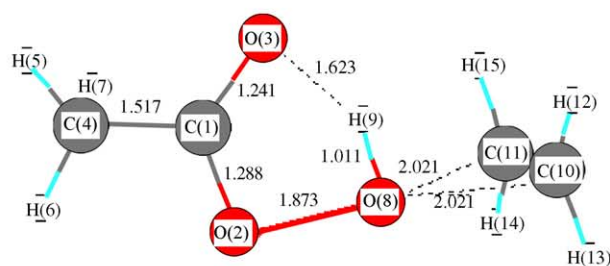
some bond angles and dihedral angles

O(3)-C(1)-O(2)	126.05	C(1)-O(2)-O(5),C(7)	81.86
C(1)-O(2)-O(5)	102.38	C(1)-O(2)-O(5),C(8)	81.87
O(2)-O(5)-H(6)	82.73	H(6)-O(5),C(7)-C(8)	91.46
		C(1)-O(2)-O(5)-H(6)	0.00

TS --- (d) [HC(OH)OOH]<sup>+</sup>---CH<sub>2</sub>=CH<sub>2</sub>

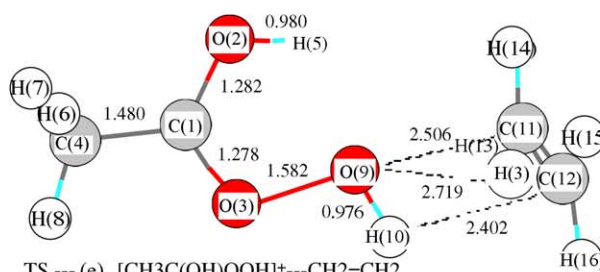
some bond angles and dihedral angles

C(1)-O(3)-O(6)	109.43	C(1)-O(3)-O(6)-H(7)	-167.33
O(3)-O(6)-H(7)	100.37	C(1)-O(3)-O(6)-C(9)	160.48
C(1)-O(2)-H(5)	112.47	C(1)-O(3)-O(6)-H(8)	-169.52

TS--- (b) CH<sub>3</sub>C(O)OOH --- CH<sub>2</sub>=CH<sub>2</sub>

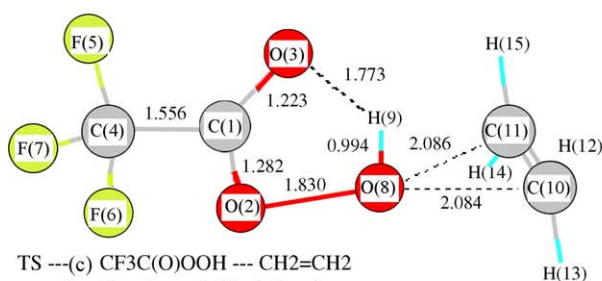
some bond angles and dihedral angles

O(3)-C(1)-O(2)	123.63	C(1)-O(2)-O(8)-H(9)	0.00
C(1)-O(2)-O(8)	102.60	C(1)-O(2)-O(8),C(10)	78.98
O(2)-O(8)-H(9)	81.30	C(1)-O(2)-O(8)-C(11)	-78.98
		H(9)-O(8),C(11)-C(10)	-91.59

TS --- (e) [CH<sub>3</sub>C(OH)OOH]<sup>+</sup>---CH<sub>2</sub>=CH<sub>2</sub>

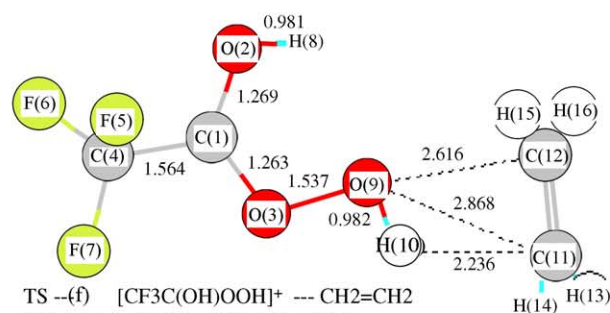
Some bond angles and dihedral angles

O(2)-C(1)-O(3)	122.62	C(1)-O(3)-O(9)-H(10)	145.99
C(1)-O(3)-O(9)	109.73	C(1)-O(3)-O(9),C(11)	-117.41
O(3)-O(9)-H(10)	98.39	C(1)-O(3)-O(9),C(12)	129.53

TS --- (c) CF<sub>3</sub>C(O)OOH --- CH<sub>2</sub>=CH<sub>2</sub>

some bond angles and dihedral angles:

O(3)-C(1)-O(2)	127.21	C(1)-O(2)-O(8)-H(9)	0.00
C(1)-O(2)-O(8)	103.95	C(10)-C(11)-O(8)-H(9)	90.80
O(2)-O(8)-H(9)	85.85		

TS --(f) [CF<sub>3</sub>C(OH)OOH]<sup>+</sup> --- CH<sub>2</sub>=CH<sub>2</sub>

some bond angles and dihedral angles:

O(2)-C(1)-O(3)	125.99	C(1)-O(3)-O(9)-H(10)	-177.41
C(1)-O(3)-O(9)	109.57	C(1)-O(3)-O(9),C(11)	-179.05
O(3)-O(9)-H(10)	101.41	C(1)-O(3)-O(9),C(12)	-178.13

Fig. 6. Transition structures (TS) of the attack of peracetic acid (a), peracetic acid (b), trifluoroperacetic acid (c) and their protonated counterparts (d–f) on ethylene. The bond distance is in angstroms, and angle is in degrees.

- (1) Bond distances of  $\text{--O--OH}$  in TS--a–c is much longer than that in TS--d–f. They are 1.872, 1.873, 1.830 and 1.546, 1.582, and 1.537, respectively. This indicates that the bond of neutral peracid must be pulled away greatly so as to enter into TS. Therefore, the reactivity of neutral peracids is much lower than that of their protonated counterparts.
- (2) For TS--a–c, The C–C bond axis of ethylene and the plane of the peracid molecules approximately are at right angles. The electrophilic oxygen atom attacks the center

of ethylene  $\pi$ -bond. The dihedral angles of the  $\pi$ -bond and  $\text{--OH}$  are 91.46, 91.59, and 91.00, respectively. However, The C–C bond axis of ethylene and the plane of the protonated peracids in TS--d–f are not at right angles. The dihedral angles (C–C–O–H) of the  $\pi$ -bond and the  $\text{--O--H}$  are 1.31, 37.70 and 1.90 degrees, respectively. This shows that the  $\pi$ -bond and the  $\text{--O--H}$  bond of protonated peracetic acid (a) and trifluoroperacetic acid (c) with high reactivity are approximately in the same plane. The electrophilic oxygen atom is not directed toward the

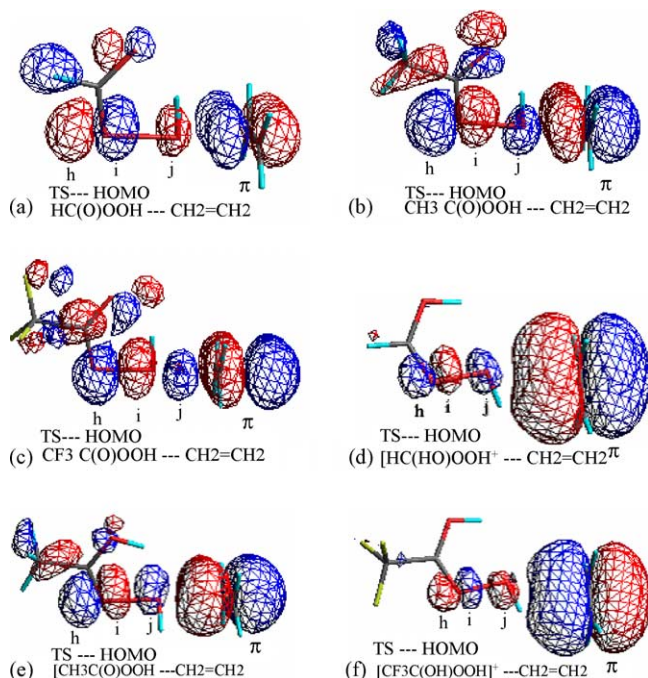


Fig. 7. HOMOs of transition structures of ethylene epoxidation by performic acid (a), peracetic acid (b), trifluoroperacetic acid (c) and their protonated counterparts (d–f) (orbital contour value = 0.03).

center of the  $\pi$ -bond. This should be attributed to the oxygen atom and hydrogen atom on the  $-\text{O}-\text{H}$  bond of protonated peracids both having strong affinity for the double bond.

### 2.6. The nature of alkene epoxidation by peracids: nucleophilic transfer of $\pi$ -electrons toward the $\sigma^*$ -orbital of peroxo bond

Recently, a quantum chemical study [6] revealed that the epoxidation with Mimonn-type diperoxomolybdenum complexes should be considered as the nucleophilic attack of the  $\pi$ -electrons of alkenes toward the  $\sigma^*$  orbital of peroxo bond. Our analysis on the transition structures and IRC calculation results confirmed that the alkene epoxidation by peracids has the identical nature.

Fig. 7 shows the HOMOs of transition structures of ethylene epoxidation by performic acid (a), peracetic acid (b), trifluoroperacetic acid (c) and their protonated counterparts (d–f). Among the four ellipsoids h, i, j and k of  $\sigma^*$  orbital of neutral or protonated peracids (see Fig. 1), k disappeared. This shows that an overlap of the double bond of ethylene with  $\sigma^*$  orbital of neutral or protonated peracids has occurred. In addition, h, i and j originally are the parts of the empty  $\sigma^*$  orbital, but now have changed to the parts of the HOMO of TS. This also proves that the  $\pi$ -electrons of ethylene has transferred into the  $\sigma^*$  orbital of the peroxo bond in TS. It is interesting to note that the volumes of i, j and k in transition structures a–c of neutral peracids are remarkably greater than those in d–f of their protonated

Table 4  
Nucleophilic transfer of  $\pi$ -electrons of ethylene toward the  $\sigma^*$  orbital of the peroxo bond in TS

TS	a	b	c	d	e	f
Total charge on ethylene	0.32	0.31	0.32	0.17	0.19	0.17
$E_{\text{HOMO}}$	-7.37	-7.13	-7.97	-12.15	-12.41	-12.25

counterparts, but the volumes of  $\pi$  orbital of ethylene in a–c are much smaller than those in d–f.

The data in Table 4 shows that the total charge on ethylene in the TSs is positive, which indicates that the transfer of  $\pi$ -electrons toward the  $\sigma^*$  orbital of the peroxo bond occurs. The degrees of electron transfer in transition structures a–c of neutral peracids are remarkably higher ( $\sim 80\%$ ) than those in d–f of their protonated counterparts. Obviously, this results in the volume differences between the orbital components in the two kinds of TS-HOMOs. The  $\sigma^*$  orbital of protonated peracids with high reactivity only need to obtain a small amount of  $\pi$ -electrons for entering into TS, but neutral peracids with low reactivity need to obtain much more  $\pi$ -electrons to be able to do so.

Table 4 also lists the orbital energies ( $E_{\text{HOMO}}$ ) of HOMO of the transition structures. A remarkable characteristic is that  $E_{\text{HOMO}}$ 's of transition structures a–c of neutral peracids are much higher than those of d–f of their protonated counterparts. This situation should be attributed to the fact that  $E_{\text{UMO}\sigma^*}$  of the  $\sigma^*$  orbital of the neutral peracids is much higher than that of their protonated counterparts (see Figs. 2 and 5). Therefore, when the same amount of  $\pi$ -electrons are transferred into the  $\sigma^*$  orbital of the peracids,  $E_{\text{HOMO}}$  of a–c systems would be higher than that of d–f. Moreover, the amount of  $\pi$ -electrons transfer amount for a–c are notably more than for d–f (Table 4).

In order to observe the electron transfer process, a reaction path calculation (IRC) on the epoxidation of ethylene by protonated performic acid has been performed. We lists some representative results of the IRC calculations (Table 5, Fig. 6), which is enough to reveal the nature of the epoxidation of alkenes by peracids.

In Table 5, the total charge on ethylene in the intermediates is positive, which proves that the transfer of  $\pi$ -electrons on double bond toward the  $\sigma^*$  orbital of peroxo bond occurs. The degree of the electron transfer in Table 5 is increased with lengthening  $-\text{O}-\text{OH}^+$  bond.

Fig. 8 shows that the HOMO graphs of the initial structure, some typical intermediates and final products obtained by IRC and single point energy or Opt calculations at the

Table 5  
IRC and single point energy calculation suggest that  $\pi$ -electrons of ethylene have transferred into the  $\sigma^*$  orbital of the peroxo bond of protonated performic acid

$-\text{O}-\text{OH}$ (Å)	1.436	1.493	1.576	1.698	1.910	2.152
Total charge on ethylene	0.129	0.139	0.197	0.322	0.546	0.771



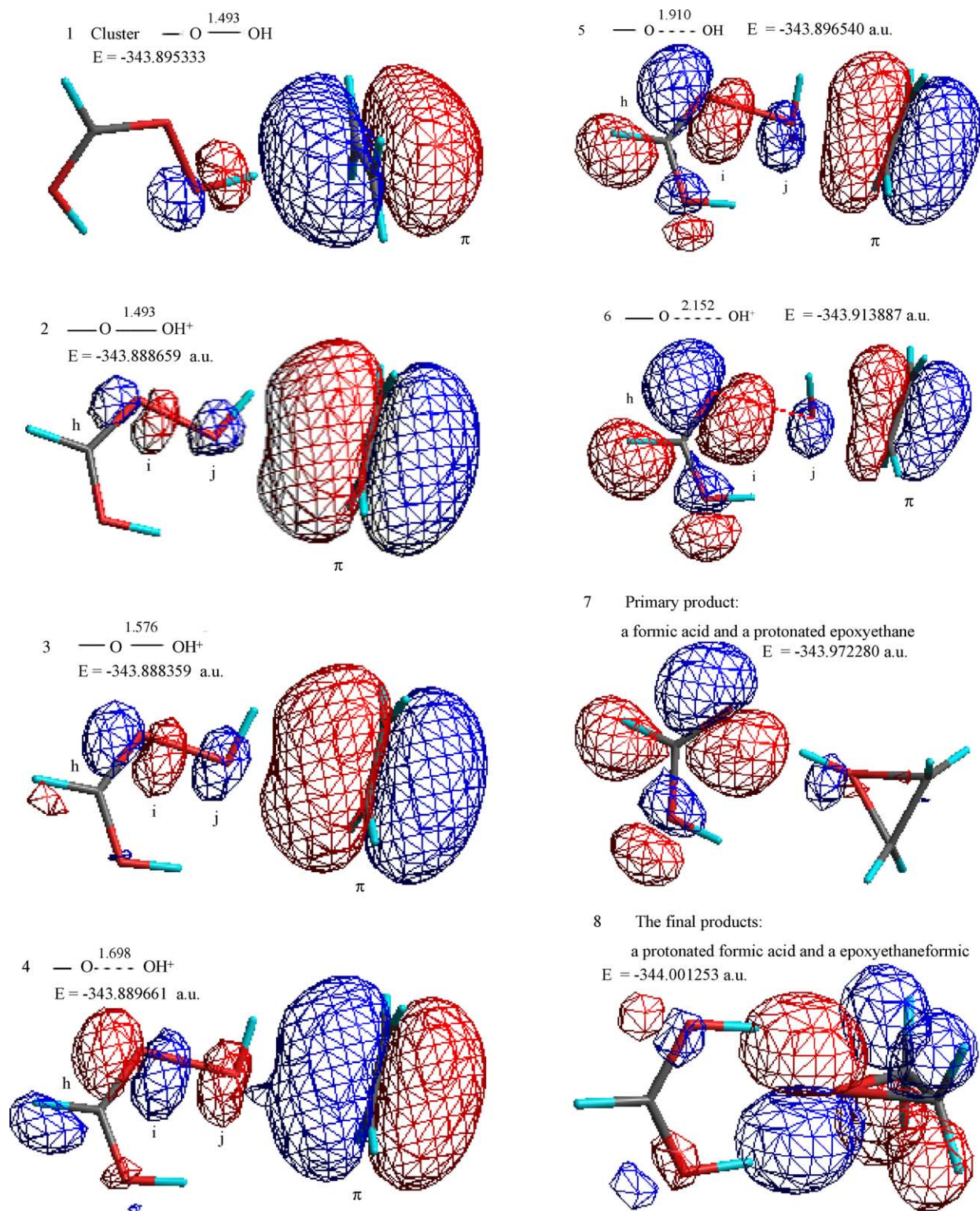


Fig. 8. HOMO graphs of the initial structure **1**, intermediates **2–7** and final product **8** in the epoxidation of ethylene by protonated performic acid. **1** and **8** were obtained by IRC and Opt calculations and **2–7** by IRC and single point energy calculations (orbital contour value **1–6** = 0.03, **7, 8** = 0.04). HOMO graph of the TS was shown in Fig. 7.

RB3LYP/6–311G(d,p) level. The IRC clearly indicates that the microscopic process of the epoxidation of alkene by peracids is a nucleophilic transfer of  $\pi$ -electrons toward the  $\sigma^*$  orbital of peroxo bond (Fig. 9).

Structure **1**. It is the HOMO graph of the initial structure. Although the total Mulliken atomic charge of ethylene is not zero in the initial structure, the electrons of ethylene have not transferred into  $\sigma^*$  orbital of the peroxo bonds.



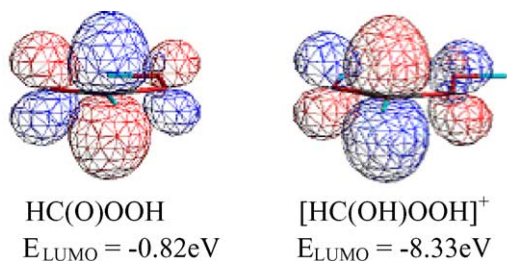


Fig. 9. The LUMO of neutral and protonated performic acid.

**Structure 2.** When the  $-\text{O}-\text{OH}$  bond length is 1.493, a small amount of  $\pi$ -electrons of ethylene has transferred into the  $\sigma^*$  orbital of the peroxy bond of protonated performic acid.

**Structure 3–6.** The h–j, three ellipsoids, become larger and larger and the their  $\pi$  orbitals become smaller and smaller. For structure **5** and **6** the  $\pi$ -electrons of double bond not only transferred into the  $\sigma^*$  orbital of peroxy bond, but also into other parts of the acid molecules. This indicates that the  $\pi$ -electrons transfer quickly increases along the extension of peroxy bond. The double bond of ethylene gradually approaches the oxygen atom of  $-\text{O}-\text{H}$  in protonated performic acid.

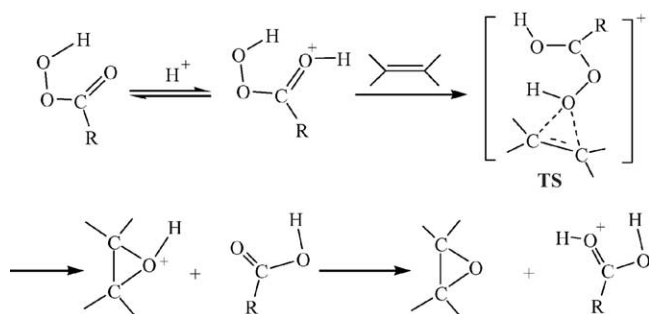
**Structure 7.** At this moment, the protonated performic acid and ethylene have changed into one formic acid molecule and one protonated epoxyethane. From **2** to **7**, ethylene continuously gives  $\pi$ -electrons to peroxy bond. In this way, ethylene finally gains the  $-\text{OH}$  of the peroxy bond and forms a protonated epoxide.

**Structure 8.** The final product is a neutral epoxyethane and a protonated formic acid. Although the primary product in the bimolecular reaction is a protonated epoxide, the  $\text{H}^+$  has finally transferred to the oxygen atom of the carbonyl group. From **7** to **8**, the total energy of the epoxidation systems has dropped by 18.17 kcal/mol. This indicates that the formations of the neutral epoxide and protonated formic acid can enhance the stability of the system. It also means that, in the acidic environment,  $\text{H}^+$  can catalyze the epoxidation but would not destroy the epoxide.

### 2.7. Mechanism of the epoxidation by peracids: a protonation-promoted process

According to the above results by DFT calculation, the mechanism of alkene epoxidation by peracid should be a protonation-promoted pathway, as shown in Scheme 3.

The protonation of neutral peracids is the key step in the epoxidation because the peracids are strongly activated. The oxygen atom transfer in the transition structure (**TS**) is also a concerted process similar to the Bartlett mechanism. The transition structure in the Bartlett mechanism is a plane consisting of double bond and peroxy acid. Our calculation results (see Figs. 6 and 7) indicate that **TS--d** and **TS--f** are approximately planar, but **TS--e** is non-planar. Hydrogen bond is important [8] in the Bartlett mechanism, but in



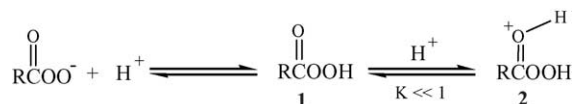
Scheme 3. Proposed mechanism of the epoxidation of alkenes by peracids.

the transition structures formed by protonated peracids, the hydrogen bond has not displayed an obvious role. IRC suggests that the primary product is a protonated epoxide, but the final product is a neutral one (Fig. 8).

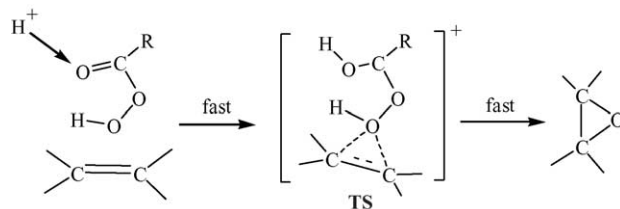
The epoxidation reactivity of a protonated peracid closely relates to its **PA**. The bigger **PA** is, the stronger the reactivity of the peroxy acid is because the protonated intermediate forms easily and has relatively long lifetime. Among them, MCPBA and PBA have higher **PA** (203.0, 206.8 kcal/mol) than the others. Although both of  $E_{\text{UMO}\sigma^*}$  (see Fig. 5) are not very low, they have good epoxidation ability and are often selected as reagent of epoxidation because of their high **PA**.

Although PBA, mCPBA and peracetic acid are weak acids, all of them can form the protonated peracids in solution because the following equilibrium would be achieved:

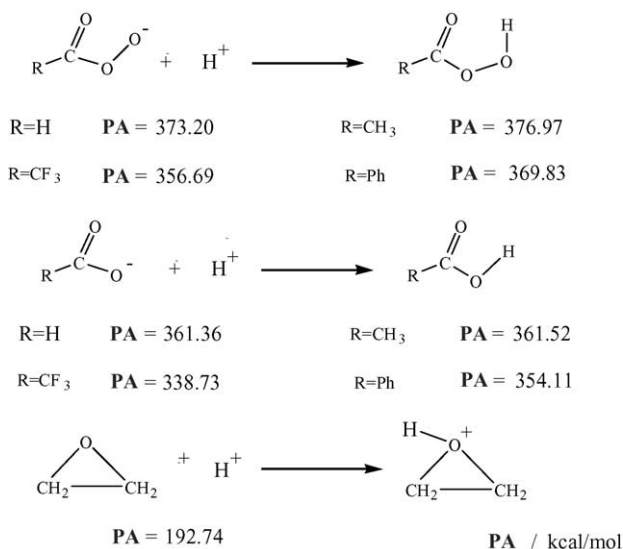
In Scheme 4, the equilibrium concentration of protonated peracids in common organic solvent must be very small ( $K \ll 1$ ) and the lifetime of the protonated species must be short. However, this does not disturb the promoting effect of protonation on the reactivity of peracids because epoxidation is an instantaneous process. For example (Scheme 5), a neutral peracid molecule is already very close to the alkene, but cannot get over the activation barrier and complete the epoxidation. At this moment, the attack of a proton to the carbonyl group makes the peracid molecule protonated, and thus gets



Scheme 4. The ionization and protonation balance of peracids generated in reaction solution.



Scheme 5. The instantaneous attack of a proton to the carbonyl group of a peracid makes the epoxidation completed at once.



Scheme 6. PA of epoxyethane and the negative ions of some peracids or acids.

over the activation barriers. The epoxidation was completed at once.

The final products are an epoxide and a protonated acid. In the process, neutral acid plays the role of a Lewis base. Actually, the negative ions of the acids or peracids are strong Lewis base. The negative ions than neutral acids or peracids have stronger affinity with H<sup>+</sup> (Scheme 6). Therefore, primary protonated epoxides fall out of the H<sup>+</sup> more easily through acting with the negative ions.

Moreover, it must be pointed out that for either a protonated or neutral peroxy acid, the UMO in which the  $\sigma^*$  orbital of peroxy bond lies is not LUMO but the next or higher UMO ( $N_{\text{UMO}\sigma^*} = +1$ , or  $+2$ ).  $E_{\text{LUMO}}$  of the LUMO is lower than  $E_{\text{UMO}\sigma^*}$ . The main component of the LUMO is a p orbital (Fig. 9) of the carbon atom in peracid. Therefore,  $\pi$ -electrons of double bond can also attack the unoccupied orbital; i.e. some side reaction would occur. Indeed, during the epoxidation by peracids, the side reactions would occur easily including the formation of rearranged byproducts and induced decomposition of peracids [10(b)]. Therefore, conditions such as temperature must be well controlled in the organic reactions using peracids; otherwise, side reaction would prevail. It seems that the origin is the LUMO of protonated peracids.

## 2.8. Explanation of some kinetic facts

Protonation is a widely observed phenomenon in the systems in which protonic acids are present, but people often overlook the important interaction. If considering protonation, some important kinetic facts on the epoxidation of alkenes by peracids could be easily understood.

(1) As early as the 1960s, Schwartz and Blumbergs [9] found that trichloroacetic acid catalyzes the rate of epoxidation

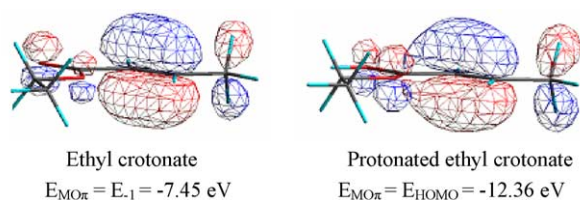


Fig. 10. Graph and  $E_{\text{MO}\pi}$  of the MO in which  $\pi$ -bonding orbital of neutral or protonated ethyl crotonate lies.

of stilbene with PBA but retards the rate of epoxidation of a double bond bearing an ester constituent like in ethyl crotonate. In addition, Renolen and Ugelstad found that no acid catalysis was observed in the PBA epoxidation of cyclohexene upon addition of dichloroacetic acid in a benzene-ether solvent system [10,2].

We propose that the kinetic phenomena should be attributed to the protonation of PBA, ethyl crotonate and ether.

When trichloroacetic acid is added into the stilbene epoxidation system, protonation of PBA would be enhanced and thus the epoxidation rate is increased. However, for the epoxidation of ethyl crotonate, both PBA and ethyl crotonate would be protonated by the strong acid. According to the calculations at the B3LYP/6-311G(d,p) level,  $E_{\text{MO}\pi}$  of ethyl crotonate in the molecular state is  $-7.45$  eV, but  $E_{\text{MO}\pi}$  of the protonated ethyl crotonate is  $-12.36$  eV (Fig. 10). Therefore, the protonation of the ester makes  $E_{\text{MO}\pi}$  drop down to  $\sim 5$  eV, which greatly reduces the reactivity of  $\pi$ -electrons in ethyl crotonate and finally makes ethyl crotonate unable to be epoxidized by protonated PBA. The carbonyl group of ester is easily protonated because it has high proton affinity (PA), for ethyl crotonate, PA = 213.2 kcal/mol (Scheme 7).

Ether also has considerably high proton affinity; for diethyl ether, PA = 196.3 kcal/mol (Scheme 7) from the calculation at the B3LYP/6-311G(d,p) level. The strong acid (in catalytic dose) could not effect protonation of the peracid because the solvent is dominant in the reaction solution. Therefore, the acid catalysis could be hardly observed for the benzene-ether solvent system.

(2) In 1997, Bach et al. [2] reported that when trifluoroacetic acid (TFCA) was used as catalyst in benzene solvent, a 6.8 fold increase in the rate of epoxidation of (*Z*)-cyclooctene (Fig. 3.  $E_{\text{MO}\pi} = E_{\text{HOMO}} = -6.39$  eV) with mCPBA ( $E_{\text{MO}\sigma^*} = -6.35$  eV) was observed. In the experiment, the level of TFCA was 1–10 equivalent of mCPBA, but was not a catalytic dose. They also calculated the clusters and transition structure of the attack of performic acid and its protonated counterpart on ethylene by DFT at the B3LYP/6-311G(d,p) level. For protonated performic acid, the activation barrier is only 4.4 kcal/mol (they did not consider zero-point correction energies of TS and the cluster). The result is identical with what we obtained for the structures and the barrier (TS--d,

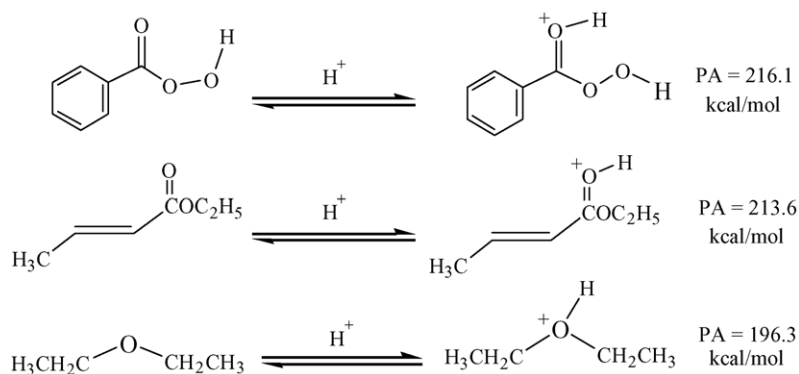
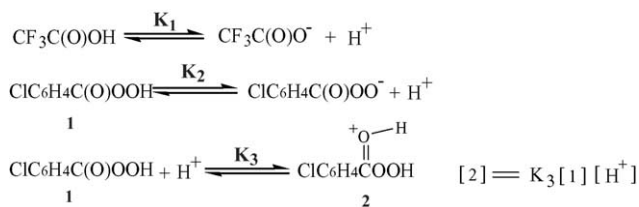


Table 3). However, they were not aware that the epoxidation by peracids should be a protonation-promoted process. They suggested that this increase in the rate was due to complexation of the peracid with the undissociated acid catalyst (HA) rather than protonation of the peracid. On contrary, we consider that the increase should be attributed to the enhanced protonation of mCPBA. According to Scheme 8, as the  $[H^+]$  increases, the [2] also increases. Therefore, the epoxidation rate would be speeded up.

TFCA dissolves in non-protonic organic solvent that is different from dissolving in water. In water, the strong acid TFCA can be fully dissociated. However, in non-protonic organic solvent, TFCA follows an equilibrium (Scheme 8) as do weak acids. The equilibrium constants are in the order  $K_1 > K_2$  (Scheme 8). This is due to the  $H^+$  and  $RCOO^-$  (cation and anion), neither of which is not “comfortable” in the solvents (such as benzene), and thus being in ionic state is not as stable as in molecular state. In organic solvents, the concentration of  $H^+$  is actually low. Therefore, its catalysis role is not as important as expected.

Perhaps, an alternative explanation of the catalytic action would exist: TFCA is oxidized by mCPBA to TFPCA and then protonated. The protonated TFPCA has much lower  $E_{UMO\sigma^*}$  ( $-7.97$  eV) and so would have much higher epoxidation reactivity than mCPBA ( $E_{UMO\sigma^*} = -6.35$  eV). However, it was proved by experiments that no such oxygen transfer takes place between a strong acid and a weak peroxy acid [11].



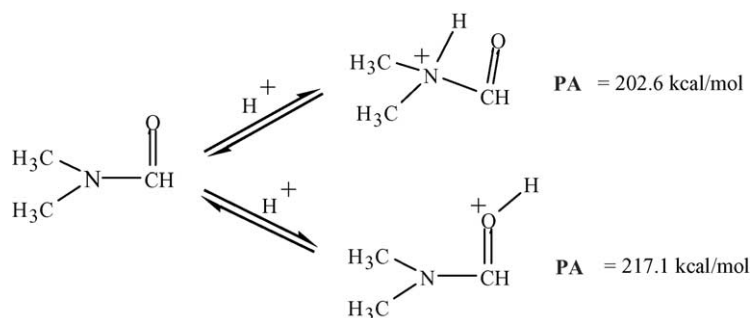
Scheme 8. The dissociation equilibrium and catalytic role of TFCA in non-protonic solvent.

- (3) A large amount of data [12] clearly shows that electro-donating groups on alkenes increase the epoxidation rate and that electron withdrawing groups on peroxy acids also increase the rate. Obviously, the electro-donating groups on alkenes can heighten the  $E_{MO\pi}$  and thus increase the reactivity of  $\pi$ -electrons of alkenes. For example,  $E_{MO\pi}$  of ethylene is  $-7.1$  eV, but that of tetramethyl ethylene is  $-6.4$  eV according to the calculation at the B3LYP/6–311G(d,p) level. The electron-withdrawing groups on a peracid can reduce the  $E_{UMO\sigma^*}$  of the peracid that increases the reactivity of the peracid. For example,  $E_{UMO\sigma^*}$  of protonated peracetic acid is  $-7.24$  eV, but  $E_{UMO\sigma^*}$  of protonated TCPA is  $-7.58$  eV and  $E_{UMO\sigma^*}$  of protonated TFPCA is  $-7.97$  eV according to the calculation at the B3LYP/6–311G(d,p) level. Furthermore, electron withdrawing groups can increase the acidity of peracids and thus increase the concentration of protonated peracid.
- (4) In the epoxidations by peracids, the influence of solvent is outstanding. Curci et al. [13] had investigated influence of various solvents on the rate in epoxidation of cyclohexene by PBA. However, they did not discover the origin of the influence. We could conclude that the protonation of some solvents is the principal origin of the influence. Basic solvent such as DMF and amine would inhibit the

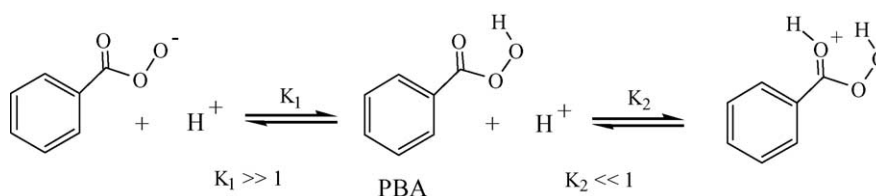
Table 6  
Epoxidation rate constants of cyclohexene by PBA in various solvents and PA of some solvents

Solvent	$10^4$ (K)	PA (kcal/mol)
CHCl <sub>3</sub>	472.0	
CH <sub>2</sub> Cl <sub>2</sub>	225.0	
CCl <sub>4</sub>	77.2	
Benzene	156.0	
Sulfolane	32.7	206.9
Dioxane	9.75	200.5
DMF	2.22	202.6, 217.1
<i>t</i> -BuOH	2.5	204.5
<i>i</i> -PrOH	6.91	200.2
EtOH	5.56	195.7
MeOH	5.44	189.0
CF <sub>3</sub> CH <sub>2</sub> OH	268	178.3





Scheme 9. DMF has two protonation sites and the strongest PA.



Scheme 10. Neutral PBA (molecular state) always is the dominant component in common solvents.

epoxidation because the solvent molecules have strong ability to combine with  $H^+$  that makes peracid hard to be protonated. In Table 6, DMF has the lowest rate (2.22) because it has two protonation sites, a nitrogen atom and an oxygen atom, and both have high proton affinity (Scheme 9). Except  $CF_3CH_2OH$ , the solvents, which are able to be protonated always have much slower epoxidation rate than the solvents ( $CHCl_3$ -benzene) which are unable to be protonated. The influence of solvents on the epoxidation rates is also related to other factors, such as molecular size, structure, component, partial charge on atoms, and polarity because they would also influence the action of the solvent on  $H^+$ . Therefore, from  $CHCl_3$  to benzene in Table 6, although all of them are unable to be protonated, the epoxidation rates in the solvents have considerable differences. Among the solvents in Table 6,  $CF_3CH_2OH$  is an exception. Although it can be protonated, the epoxidation rate in the solvent is high. The major reason is that the alcohol has strong acidity and thus can increase the protonation of PBA.

Neutral PBA is a weak acid. The dissociation of PBA in the solvents in Table 6 is small, even if in DMF. Therefore, if the epoxidation has been completed by neutral PBA, the rate of epoxidation in the solvents should not have significant change because PBA in molecular state is always the dominant component (Scheme 10,  $K_1 \gg 1$ ). However, the influence of different solvents on the protonation of PBA is significant. For some solvents, such as DMF, originally less  $H^+$  from PBA is now used for protonating a large number of the solvent molecules, which makes the protonation of PBA negligible. Therefore, the great changes of the rate constants in different solvents (Table 6) just prove that the epoxidation occurs by way of protonated PBA.

### 3. Conclusion

This study reveals that the epoxidation of alkene by peracids is a protonation-promoted pathway. The importance of the protonation is that both  $E_{UMO\sigma^*}$  of the UMO in which the  $\sigma^*$  orbital of peroxy bond of peroxy acids lies and activation barriers  $\Delta E^*$  of the epoxidation drop significantly. The  $E_{UMO\sigma^*}$  of the protonated peracids is in the same as or even lower level than  $E_{MO\pi}$  of alkenes, which makes the epoxidation easily initiated and completed. The study also confirms that the nature of the epoxidation of olefin by peracids is nucleophilic transfer of  $\pi$ -electrons of alkene toward the  $\sigma^*$  orbital of peroxy bond in peracids. Based on this mechanism, some important kinetic facts of alkene epoxidation by peracids are easily elucidated.

### Acknowledgments

We are grateful to the Institute of Medical Science, Tsinghua University, for financial support of this research and to Professor Guoshi Wu, Institute of Physical Chemistry, Tsinghua University, for effective support and comments on quantum chemical calculation.

### References

- [1] (a) P.D. Bartlett, *Rec. Chem. Prog.* 11 (1950) 47;  
(b) P.D. Bartlett, *Rec. Chem. Prog.* 18 (1957) 111.
- [2] R.D. Bach, C. Canepa, J.E. Winter, P.E. Blanchette, *J. Org. Chem.* 62 (1997) 5191.
- [3] (a) J.O. Edwards, in: J.O. Edwards (Ed.), *Peroxide Reaction Mechanisms*, Wiley, New York, 1962, p. 67;

- (b) T. Yonezaws, H. Kato, O. Yamamoto, *Bull. Chem. Soc. Jpn.* 40 (1967) 307;
- (c) B. Plesnicar, M. Tasevski, A. Azman, *J. Am. Chem. Soc.* 100 (1978) 743;
- (d) K.W. Woods, P. Beak, *J. Am. Chem. Soc.* 113 (1991) 6281.
- [4] (a) R.D. Bach, C. Esteves, J.E. Winter, M.N. Glukhovtsev, *J. Am. Chem. Soc.* 120 (1998) 680;
- (b) R.D. Bach, P.Y. Ayala, H.B. Schlegel, *J. Am. Chem. Soc.* 118 (1996) 12758;
- (c) C. Kim, T.G. Traylor, C.L. Perrin, *J. Am. Chem. Soc.* 120 (1998) 9513;
- (d) K.J. Sea, J.S. Kim, *J. Am. Chem. Soc.* 114 (1992) 3044;
- (e) M. Freccero, R. Gandolfi, M. Sarzi-Amade, A. Rastelli, *J. Org. Chem.* 65 (2000) 8948;
- (f) M. Freccero, R. Gandolfi, M. Sarzi-Amade, A. Rastelli, *J. Org. Chem.* 65 (2000) 2030;
- (g) M. Freccero, R. Gandolfi, M. Sarzi-Amade, A. Rastelli, *J. Org. Chem.* 64 (1999) 3853;
- (h) S. Yanabe, C. Condou, T. Minato, *J. Org. Chem.* 61 (1996) 616.
- [5] Gaussian 98, Revision A.9, M.J. Frisch, G.W. Trucks, H.B. Schlegel, G.E. Scuseria, M.A. Robb, J.R. Cheeseman, V.G. Zakrzewski, J.A. Montgomery, Jr., R.E. Stratmann, J. C. Burant, S. Dapprich, J.M. Millam, A.D. Daniels, K.N. Kudin, M.C. Strain, O. Farkas, J. Tomasi, V. Barone, M. Cossi, R. Cammi, B. Mennucci, C. Pomelli, C. Adamo, S. Clifford, J. Ochterski, G.A. Petersson, P.Y. Ayala, Q. Cui, K. Morokuma, D.K. Malick, A.D. Rabuck, K. Raghavachari, J.B. Foresman, J. Cioslowski, J.V. Ortiz, A.G. Baboul, B.B. Stefanov, G. Liu, A. Liashenko, P. Piskorz, I. Komaromi, R. Gomperts, R.L. Martin, D.J. Fox, T. Keith, M.A. Al-Laham, C.Y. Peng, A. Nanayakkara, M. Challacombe, P.M.W. Gill, B. Johnson, W. Chen, M.W. Wong, J.L. Andres, C. Gonzalez, M. Head-Gordon, E.S. Replogle, J.A. Pople, Gaussian, Inc., Pittsburgh PA, 1998.
- [6] (a) D.V. Deubel, J. Sundermeyer, G. Frenking, *J. Am. Chem. Soc.* 122 (2000) 10101;
- (b) Dirk V. Deubel, J. Sundermeyer, G. Frenking, *Eur. J. Inorg. Chem.* (2001) 1819;
- (c) I.V. Yudanov, C. Di Valentin, P. Gisdakis, N. Rösch, *J. Mol. Catal. A: Chemical* 158 (2000) 189;
- (d) C. Di Valentin, P. Gisdakis, I.V. Yudanov, N. Rosch, *J. Org. Chem.* 65 (2000) 2996;
- (e) A. Hroch, G. Gemmecker, W.R. Thiel, *Eur. J. Inorg. Chem.* (2000) 1107;
- (f) C. Di Valentin, P. Gisdakis, I.V. Yudanov, N. Rösch, *J. Org. Chem.* 65 (2000) 2996;
- (g) P. Gisdakis, N. Rösch, *Eur. J. Org. Chem.* (2001) 719;
- (h) P. Gisdakis, I.V. Yudanov, N. Rösch, *Inorg. Chem.* 40 (2001) 3755.
- [7] H. Shi, G. Chen, X. Wang, Z. Zhang, X. Hong, *J. Mol. Catal. A: Chemical* 216 (2004) 29.
- [8] (a) H. Kropf, M.R. Yazdanbakhsh, *Tetrahedron* 30 (1974) 3455;
- (b) R. Curci, R.A. Diprete, J.O. Edwards, J. Modena, *J. Org. Chem.* 35 (1970) 740;
- (c) R. Kaveie, B. Plesnicar, *J. Org. Chem.* 35 (1970) 2033.
- [9] (a) N.N. Schwartz, J.H. Blumbergs, *J. Org. Chem.* 29 (1964) 1976;
- (b) G. Berti, F. Botturi, *J. Org. Chem.* 25 (1960) 1286;
- (c) G. Berti, F. Botturi, *Gazz. Chim. Ital.* 89 (1959) 2380.
- [10] P. Renolen, J. Ugelstad, *J. Chim. Phys.* 57 (1960) 634.
- [11] (a) M.F. Hawthorne, W.D. Emmons, K.S. McCallum, *J. Am. Chem. Soc.* 80 (1958) 6393;
- (b) D.R. Campbell, J.O. Edwards, J. Maclachlan, K. Polgar, *J. Am. Chem. Soc.* 80 (1958) 5308.
- [12] (a) N.N. Schwartz, J.H. Blumbergs, *J. Org. Chem.* 29 (1964) 1976;
- (b) M. Vilka, *Bull. Soc. Chim. Fr.* (1959) 1401;
- (c) H.O. Hous, R.S. Ro, *J. Am. Chem. Soc.* 80 (1958) 2428;
- (d) Y. Ogata, I. Tabushi, *J. Am. Chem. Soc.* 83 (1961), 3440, 3444;
- (e) R. Curci, R.A. Di Prete, J.O. Edwards, G. Modena, *J. Org. Chem.* 30 (1970) 740;
- (f) D. Swern, *Organic peroxides*, 2, Wiley Interscience, New York, 1971.
- [13] R. Curci, R.A. Diprete, J.O. Edwards, G. Modena, *J. Org. Chem.* 35 (1970) 740.